Journal of Signal and Information Processing, **2012, 3, 98-108**
http://dx.doi.org/10.4236/jsip.2012.31013 Published Online February 2012 (http://www.SciRP.org/journal/jsip)

A New Fast Iterative Blind Deconvolution Algorithm

Mamdouh F. Fahmy[1], Gamal M. Abdel Raheem[1], Usama S. Mohamed[1], Omar F. Fahmy[2]

[1]Department Electrical Engineering, Assiut University, Assiut, Egypt; [2]Department of Electrical Engineering, Future University, Cairo, Egypt.
Email: omarfarouk_mamdouh@hotmail.com

Received December 8th, 2011; revised January 9th, 2012; accepted January 18th, 2012

ABSTRACT

Successful blind image deconvolution algorithms require the exact estimation of the Point Spread Function size, PSF. In the absence of any priori information about the imagery system and the true image, this estimation is normally done by trial and error experimentation, until an acceptable restored image quality is obtained. This paper, presents an exact estimation of the PSF size, which yields the optimum restored image quality for both noisy and noiseless images. It is based on evaluating the detail energy of the wave packet decomposition of the blurred image. The minimum detail energies occur at the optimum PSF size. Having accurately estimated the PSF, the paper also proposes a fast double updating algorithm for improving the quality of the restored image. This is achieved by the least squares minimization of a system of linear equations that minimizes some error functions derived from the blurred image. Moreover, a technique is also proposed to improve the sharpness of the deconvolved images, by constrained maximization of some of the detail wavelet packet energies. Simulation results of several examples have verified that the proposed technique manages to yield a sharper image with higher PSNR than classical approaches.

Keywords: Blind Image Deconvolution; Image Enhancement

1. Introduction

The goal of blind deconvolution is to recover two convolved signals *f* and *h* from their convolved (*and normally noisy*), version *g*. Neither *f* nor *h* is known. In image processing, *f* represents the true image, whereas *h* represents the Point Spread Function PSF, which is responsible for blurring *f*. Even if we have a priori information about the PSF, recovering the original image by inverse filtering is usually counterproductive, as it involves noise amplification, [1,2]. At this point it is worth mentioning that, not all blurring causes can be precisely determined. In general, the PSF can be described by the 2D Gaussian as in atmospheric turbulence or by circular PSF as in defocusing effects [3]. However, Central limit theorem implies that receiving blurred version of the image is closer to blurring the original image by a Gaussian distribution PSF. Note that the Gaussian PSF is one of the most difficult cases to deal with in blind deconvolution, as it can be factored into two Gaussian PSF. In the noiseless case $g = h^{**} f$. Solution starts by choosing an initial guess of *f*, (*normally taken to be the blurred image itself*), then obtain *h* as the least squares solution of $\|g - h^{**} f\|$. Iteration is reversed and we seek to estimate *f* using the estimated *h*. However, as the size of *h* is much smaller than *f*, this approach is computationally prohibitive. Many efficient techniques have been proposed to solve this problem, [4-9]. In [4], an Iterative Blind Deconvolution technique *IBD* has been proposed by alternate updating the 2-D FFT of *f* and *h*, until the relation $G(\omega_1,\omega_2) \cong F(\omega_1,\omega_2)H(\omega_1,\omega_2)$, is almost satisfied. In its initial versions, it suffered from poor convergence, yet in latter versions [5], its robustness to noise and convergence properties are highly improved. An alternate double iteration algorithm that has good anti-noise capability has also been described in [6, 7]. It is known as the Richards-Lucy algorithm, and is characterized with robustness to either Poisson or Gaussian noise, [8,9]. In [5-10], a thorough treatment of different blind deconvolution techniques can be found. All these techniques require an exact estimation of the blurring PSF size. In view of the absence of any priori information about the PSF size, the application of the IBD, Richards-Lucy or any other blind deconvolution algorithms will fail to yield good quality restored images. This paper, addresses this problem. It shows how the optimum blurring size, can be accurately estimated for both noisy and noiseless images. Then, using this estimated PSF size the performance of IBD, RL or any other blind deconvolution algorithm is further improved. This improvement is achieved by iterating between updating the restored image $\hat{f}(m,n)$ and the PSF $\hat{h}(m,n)$ that minimizes some arbitrary largest absolute error devia-

tions of the error $e(m,n)=g(m,n)-\hat{g}(m,n)$ where $\hat{g}=\hat{h}\otimes\hat{f}$. Further, the paper also describes a technique for improving the sharpness of the deconvolved image, through maximizing some of the wavelet packet detail energies, while minimizing the residual reconstruction error energy. Simulation results of several images blurred by Gaussian or circular PSF, have verified that the proposed techniques substantially improve the quality of the restored images.

2. The Fast Iterative Blind Deconvolution Algorithm

2.1. Mathematical Preliminaries

If the original image *f* of size $M\times N$ is blurred by an unknown transfer function *h* of size $J\times K$, then the blurred image *g* is computed as

$$g(m,n)=\sum_{k=0}^{J-1}\sum_{j=0}^{K-1}h(k,j)\,f(m-k,n-j)+w(m,n) \quad (1)$$

w(*m*,*n*) is the associated zero—mean additive noise. For simplicity, let $M = N$, $J = K = N_p$. Using circular convolution properties, overlap is avoided if *e*ach row vectors of *f*, *g* and *w* is padded by zeros to make its length equals M_0, *where* $M_0 = M + N_p - 1 = N_0$. So, if *f*, *g* and *w* represent $M_0N_0\times 1$ column vectors formed by stacking the rows of the extended matrices, Equation (1) can be expressed as

$$g = Hf + w \quad (2)$$

H is the block circulant $M_0N_0\times M_0N_0$ matrix, defined by

$$H=\begin{bmatrix} H_0 & H_{M_0-1} & .... & H_1 \\ H_{1_1} & H_0 & .... & H_2 \\ . & & & .... \\ .... & & & \\ H_{N_0-1} & H_{N_0-2} & .... & H_0 \end{bmatrix} \quad (3a)$$

$$H_j=\begin{bmatrix} h_e(j,0) & h_e(j,N_0-1) & .... & h_e(j,1) \\ h_e(j,1) & h_e(j,0) & .... & h_e(j,2) \\ . & & & .... \\ .... & & & \\ h_e(j,N_0-2) & h_e(j,N_0-1) & .... & h_e(j,0) \end{bmatrix} \quad (3b)$$

Equation (2), suggests that, *f* can be recovered as

$$f=\left(H^tH\right)^{-1}H^t(g-w) \quad (4)$$

This equation indicates that even in case of prior knowledge of *h* and *w*, the inverse of $\left(H^tH\right)$ apart from requiring huge amount of computation for ordinary sized images, can result in an unbounded perturbation in the solution *f*. This problem is solved by taking the 2-D FFT of both *h* and *f*, as is explained in the next section.

2.2. The Constrained Lest Squares Error Algorithm

The constrained least squared error algorithm [1,2], uses the 2-D FFT techniques, to obtain the restored image. It aims to obtaining a restored image $\hat{f}(m,n)$ that is the solution of the following constrained optimization problem: Find the optimum $\hat{f}(m,n)$, $\hat{h}(m,n)$ that minimize the objective function *J*,

Minimize

$$J=\left|Q(\omega_1,\omega_2)\hat{F}(\omega_1,\omega_2)\right|^2 \ \text{for all} -\pi\le(\omega_1,\omega_2)\le\pi$$

Subject to

$$\left|G(\omega_1,\omega_2)-\hat{H}(\omega_1,\omega_2)F(\omega_1,\omega_2)\right|^2\le\varepsilon^2 \quad (5)$$

$$\hat{H}(\omega_1,\omega_2)=\sum_{m=0}^{M_1-1}\sum_{n=0}^{N_1-1}\hat{h}(m,n)\mathrm{e}^{-j(m\omega_1+n\omega_2)},$$

$$\hat{F}(\omega_1,\omega_2)=\sum_{m=0}^{M_2-1}\sum_{n=0}^{N_2-1}\hat{f}(m,n)\mathrm{e}^{-j(m\omega_1+n\omega_2)}$$

Using the Lagrange multiplier technique, this problem can be formulated as

Minimize

$$J=\left|Q(\omega_1,\omega_2)\hat{F}(\omega_1,\omega_2)\right|^2 +\lambda\left(\left|G(\omega_1,\omega_2)-\hat{H}(\omega_1,\omega_2)\hat{F}(\omega_1,\omega_2)\right|^2\right)-\varepsilon^2 \quad (6)$$

The solution to this constrained minimization problem, can be shown to be

$$\hat{F}(\omega_1,\omega_2)=\frac{\lambda\hat{H}^*(\omega_1,\omega_2)G(\omega_1,\omega_2)}{\left|Q(\omega_1,\omega_2)\right|^2+\lambda\left|\hat{H}(\omega_1,\omega_2)\right|^2} \quad (7)$$

Now, the function $Q(\omega_1,\omega_2)$ is chosen to boost the high frequency energies of $\hat{F}(\omega_1,\omega_2)$. As all natural images have pre-dominant low frequency content, minimizing *J* means that the true image $f(m,n)$ is obtained, or at least nearly obtained. *Q* can be chosen in many different ways. In [1], two formulas were given to $q(m,n)$ to approximate Laplacian function. In this paper, a simpler of $Q(\omega_1,\omega_2)$ that satisfies the high frequency emphasis requirements, is proposed. It is chosen as $Q(\omega_1,\omega_2)=\dfrac{1}{\hat{F}(\omega_1,\omega_2)}$. Using this choice, leads to the following iterative restoration algorithm

$$\hat{F}(\omega_1,\omega_2)=\frac{H^*(\omega_1,\omega_2)}{\dfrac{\alpha}{\hat{F}^{(k-1)}(\omega_1,\omega_2)}+\left|H(\omega_1,\omega_2)\right|^2} \quad \alpha=\frac{1}{\lambda} \quad (8)$$

This is precisely the update algorithm cited without proof in [4]. There, it is proposed to apply this update formula to estimate $\hat{H}(\omega_1,\omega_2)$. This results in the so-called Iterative Blind Deconvolution algorithm, *IBD*. It is an improved version of the original Iterative Deconvolution described [3], and overcome many of its shortcomings. This algorithm is implemented using the MatLab function *deconvblind*.

Now, the success of the IBD algorithm, as well as many other iterative deconvolution algorithms in estimating the original images depends on the precise estimation of the PSF order. The next section shows how this order is precisely estimated, in view of no priori information about the PSF order.

2.3. PSF Size Estimation

All iterative blind deconvolution algorithms require an estimate of the PSF size. To our knowledge, this is done on trial and error basis until good quality restored image is obtained. An analytical method is now given to estimate the optimum PSF size.

To analyze this problem, let the estimated PSF and image, be

$$\hat{h}(m,n) = h(m,n) + \delta h(m,n),$$
$$\hat{f}(m,n) = f(m,n) + \delta f(m,n)$$

where $f(m,n)$ and $h(m,n)$ are the original image and the true PSF filter. Note that in all blind deconvolution algorithms, $\delta h(m,n)$ controls $\delta f(m,n)$. So, the blurred received image $g(m,n)$, is given by

$$\begin{aligned} g(m,n) &= \hat{h}(m,n) ** \hat{f}(m,n) \\ &= \left(h(m,n) + \delta h(m,n)\right) ** \left(f(m,n) + \delta f(m,n)\right) \\ &= h(m,n) ** f(m,n) + e(m,n) \end{aligned} \quad (9)$$

Clearly, due to the uncertainty of $h(m,n), e(m,n)$ can be considered as additive noise. It mainly affects the high frequency energy bands of the image. As the perturbation $\delta h(m,n)$ gets smaller, their energy contribution to *e*(*m*,*n*) becomes smaller. This suggests to decompose *e*(*m*,*n*) using *n*-level wavelet packet decomposition and compute the detail energy in the last (*high*) wavelet packet WP_n.

If the blurred image is contaminated with zero mean AWGN, then the blurred noisy image has to be de-noised prior to PSF order estimation. The threshold level is computed as, [11]

$$T = \sigma\sqrt{2\log_e N} \quad (10)$$

σ^2 is the variance of the WP_n. It is determined through estimating its *pdf* distribution as described in [12]. *N* is its length when converted to a column vector. The following example, illustrates PSF estimation in both the noiseless and noisy cases, for Gaussian and circular defocusing blurring filters

Ex. 1:

The proposed PSF order estimation method is verified by the following simulations. The test images used, are blurred using 8 × 8 Gaussian filter with $\sigma^2 = 10$, and circular averaging filter (pillbox), with radius *r* = 3. For an arbitrary PSF order, the program estimates the deblurred image, using the Matlab function *deconvblind, or deconvlucy.* The parameters of these algorithms are: Number of cycles = 40, Threshold $\varepsilon = 0.005$, The error signal *e*(*m*,*n*) is decomposed using 2-level "*sym*4" wavelet decomposition. **Figure 1** shows the behavior of the detail energy of the *HH* sub-band with different PSF order, for these blurred images. This precise PSF estimation subsequently leads to a significant improvement restored image quality, as will be shown in the following section.

In the noisy case, the blurred image is contaminated with zero mean AWGN of $\sigma^2 = 0.01$. The blurred noisy image variances *are* [0.0557 0.0421 0.0265], respectively. In order to de-noise this noisy image, it is decomposed with 2-level "*sym*4" wavelet decomposition. The probability distribution function *pdf*, of the last *HH* wavelet packet is computed using the Bspline *pdf* estimation technique proposed in [12], using 3-level cubic Bspline wavelet with 128 histogram bins. **Figure 2**, compares the *pdf* of the *HH* sub-band with Gaussian random variable distribution having the same mean and variance. It also shows detail energy performance for both Gaussian and circular blurring PSF. Again, this figure shows that apart from accurately estimating the *pdf*, it yields the optimum PSF size for further deblurring.

2.4. The Proposed Fast Iterative Blind Deconvolution Algorithm

The proposed Fast Iterative Blind Deconvolution algorithm FIBD, is initialized by estimating the PSF order, as described above using rough estimations of the original image provided by available algorithms, (like *deconvblind*, *deconvlucy*,⋯). Having estimated the blurring PSF order, the algorithm iterates between updating the restored image $\hat{f}(m,n)$ and the PSF $\hat{h}(m,n)$. The update is based on minimizing some arbitrary M_x largest absolute error deviations of $e = \left|g - \hat{h} ** \hat{f}\right|$. The algorithm works in the spatial domain and is summarized as follows:

1) For the k^{th} estimate, evaluate $\hat{g} = \hat{h}_k ** \hat{f}_k$. Evaluate *H* from $\hat{h}$ as in Equations (3a) and 3(b). Evaluate the error $\Delta g = g - \hat{g}$. Arrange Δg in a vector form.

2) Sort $|\Delta g| = |g - \hat{g}|$ in ascending order using the

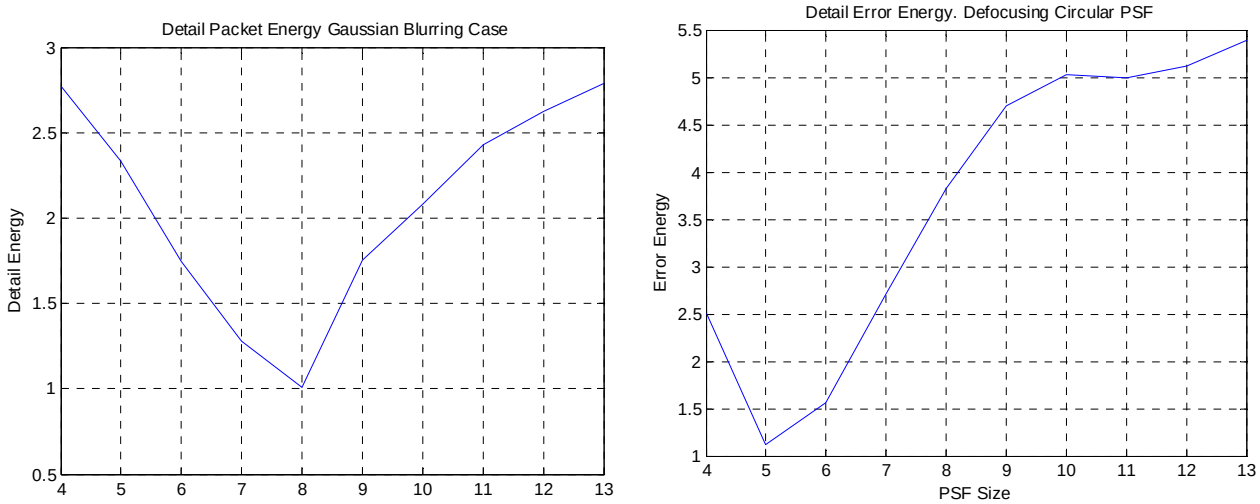

(a)

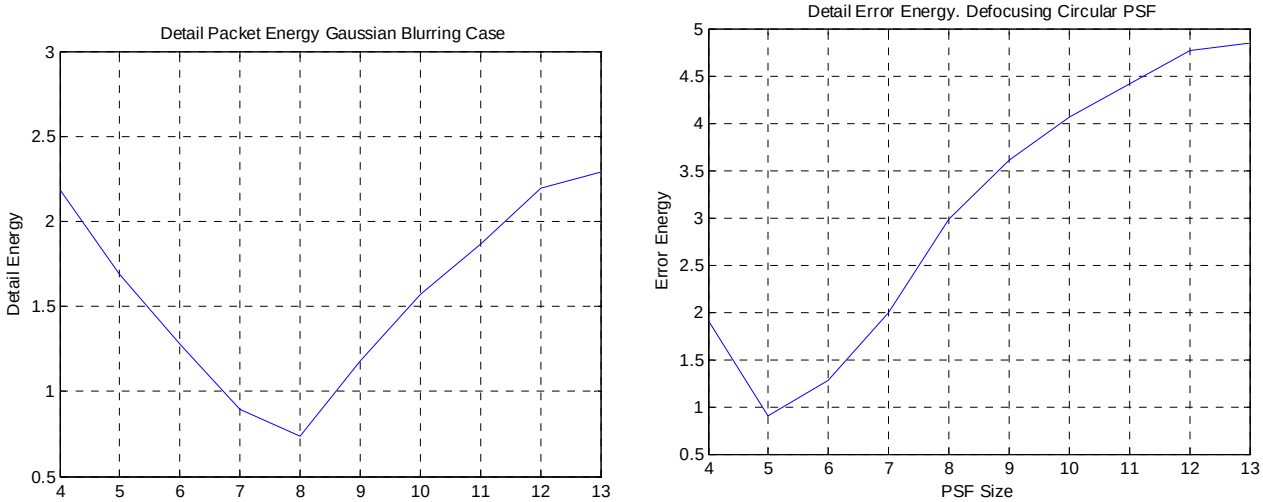

(b)

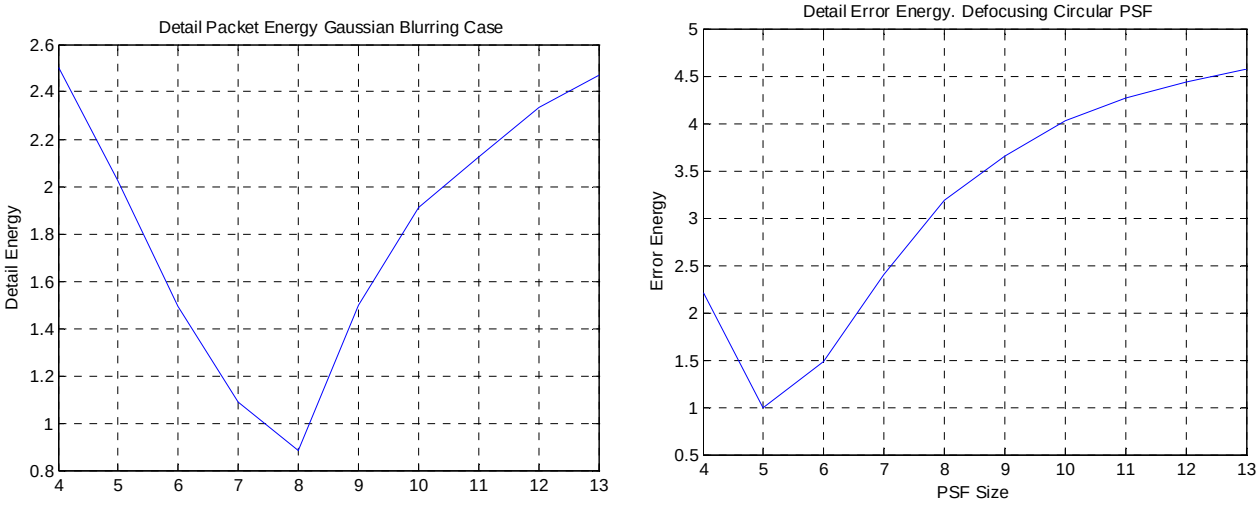

(c)

Figure 1. The detail energy of the *HH* sub-band for (a) Cameraman; (b) Lena; (c) Mandrill.

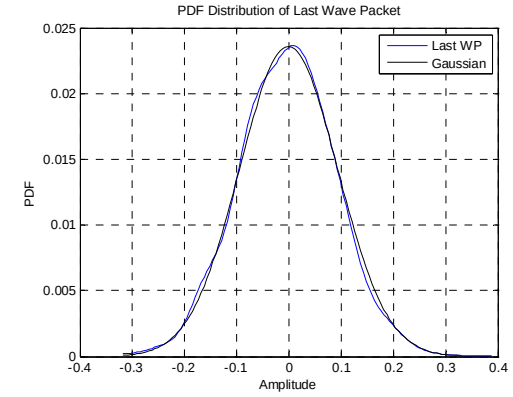

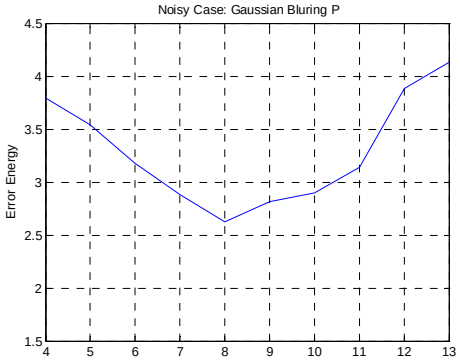

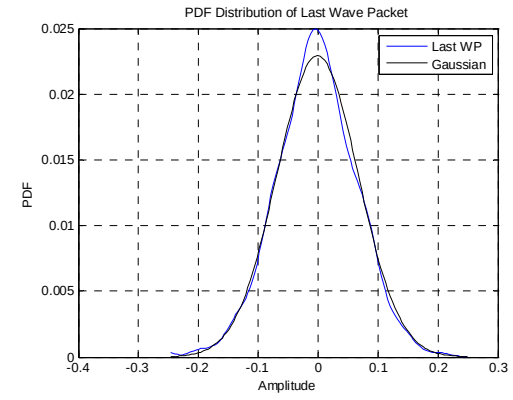

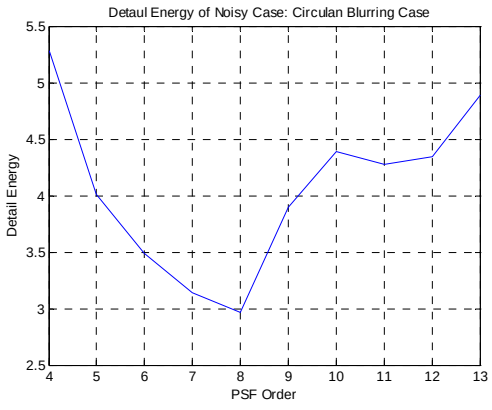

(a)

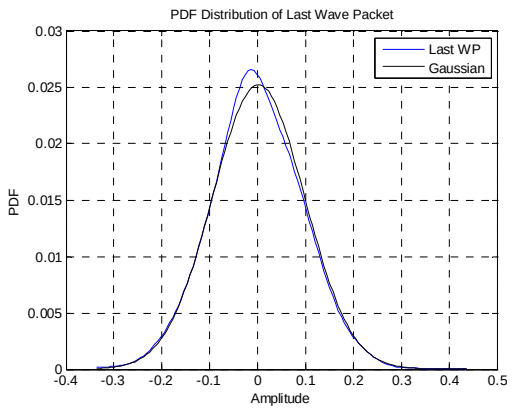

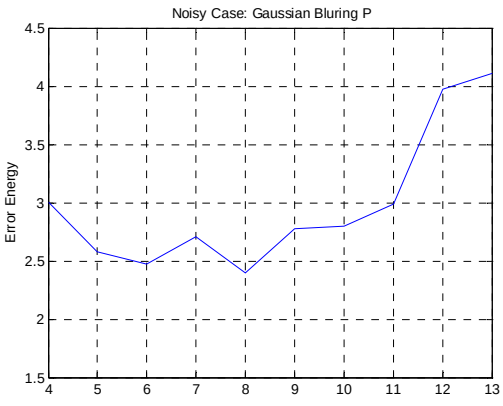

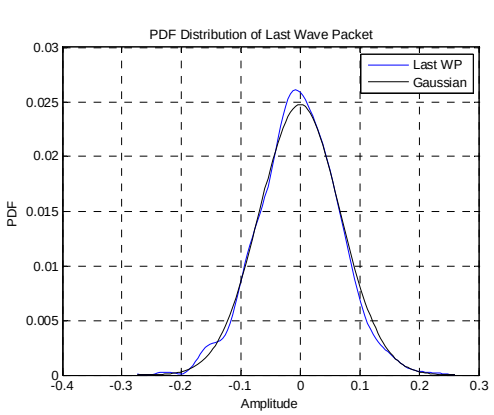

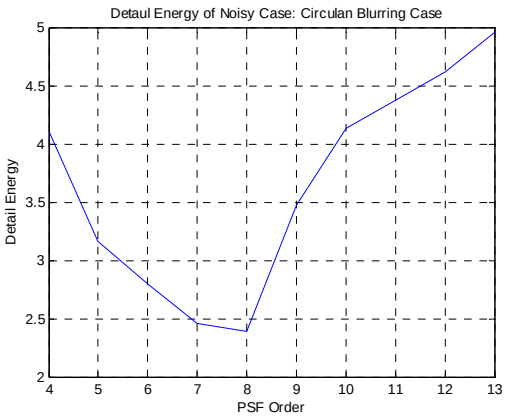

(b)

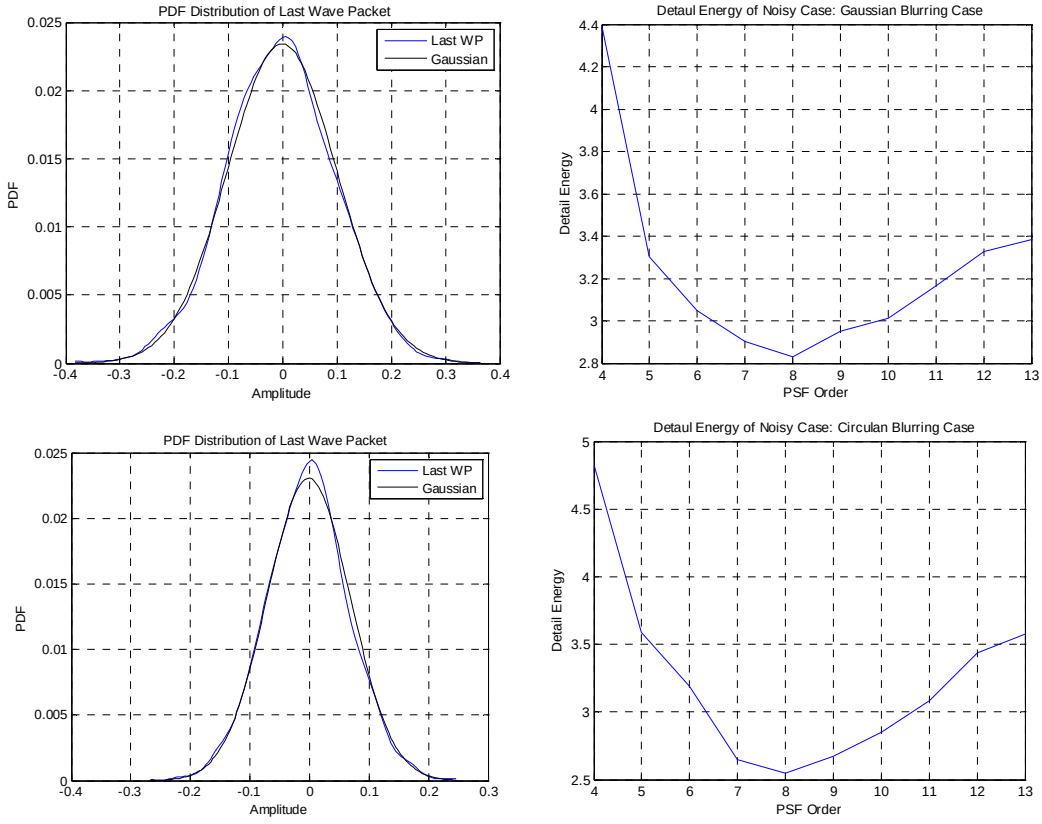

(c)

Figure 2. The *pdf* of the *HH* sub-band & detail energy performance for both Gaussian and circular blurring PSF. (a) Cameraman; (b) Lena; (c) Mandrill.

Matlab command $[V_x, I_{xm}] = sort(|\Delta g|)$. Subsequently, Sort $H^{(k)}$ as $H_s = H^{(k)}(I_{xm}, I_{xm})$.

3) For a prescribed number M_x, pick the M_x largest deviations of M_x. Denote by

$$\Delta g_{M_x} = \Delta g\left(I_{xm}(end - M_x + 1 : end)\right).$$

$$\text{Partition } H_s = \begin{bmatrix} H_{11} & H_{12} \\ H_{21} & H_{22} \end{bmatrix} \begin{matrix} \updownarrow M_x \\ \leftrightarrow M_x \end{matrix}$$

4) Only update $\hat{f}^{(k)}_{M_x}$ responsible for the M_x largest deviations of M_x. The update increments together with the updated $|\Delta g_{M_x}|$, are given by

$$-\Delta g = \begin{bmatrix} H_{12} \\ H_{22} \end{bmatrix} \Delta f^{(k)}_{M_x} \qquad (11)$$

$$f^{(k+1)} = f^{(k)} + \left[zeros(M_0 N_0 - M_x); \Delta f^{(k)}_{M_x} \right]$$

This concludes the image restoration cycle.

Updating $\hat{h}^{(k)}$ proceeds similarly through minimizing the energy of $\|g - \hat{g}\|$ using the updated image $\hat{f}^{(k+1)}(m,n)$. This update can easily be achieved either through minimizing the objective function $\zeta = \sum_m \sum_n e^2(m,n)$, $e = g - \hat{h} ** \hat{f}$ or more simply as the least squares solution of Equation (4), when h and f are interchanged.

Ex. 2:

The blurred images of Ex. (1), are deconvolved through minimizing the largest M_x peak deviations of the absolute error of $e(m,n)$. **Tables 1(a)** and **(b)** compare the PSNR improvements of the proposed *FIBD* technique, over the standard *deconvlucy* (*RL*) and *deconvblind* (*IBD*) algorithms for both 8 × 8 Gaussian and Circular PSF with $r = 3$ filters.

These tables indicate that the proposed FIBD algorithm yields a significant PSNR improvement, over the standard RL and IBD algorithms. This is due to the fact that the algorithm modifies pixels responsible for the severest image degradation, unlike other methods using 2-D FFT that considers all parts of the image to have equal importance. **Figures 3-5**, show the rate of convergence as well as the deconvolved images, for the Gaussian blurring filter, whereas **Figure 6** illustrated the blurring and deconvolved images in the circular blurring case. To end this section, it is worth pointing out that, if the PSF size is chosen different from the value estimated in the previous section, severe degradation of the quality of

Table 1. (a) Gaussian PSF.

	RL	IBD	FIBD				
			M_x = 64	128	256	512	1024
Cameraman	23.5290	23.6468	25.0114	25.1386	25.3356	25.5039	25.6131
Lena	24.8168	25.1177	25.6029	25.7005	25.8791	25.8991	26.1026
Mandril	22.0956	22.3211	23.1868	23.3061	23.3616	23.5978	23.5822

Table 1. (b) Circular PSF (defocusing).

	RL	IBD	FIBD				
			M_x = 64	128	256	512	1024
Cameraman	25.7076	25.6617	26.3235	26.4553	26.6151	26.6542	26.6373
Lena	27.2209	27.2219	27.5423	27.7395	27.8868	28.0509	28.0413
Mandril	24.0190	23.7927	24.3658	24.4249	24.5135	24.6128	24.6197

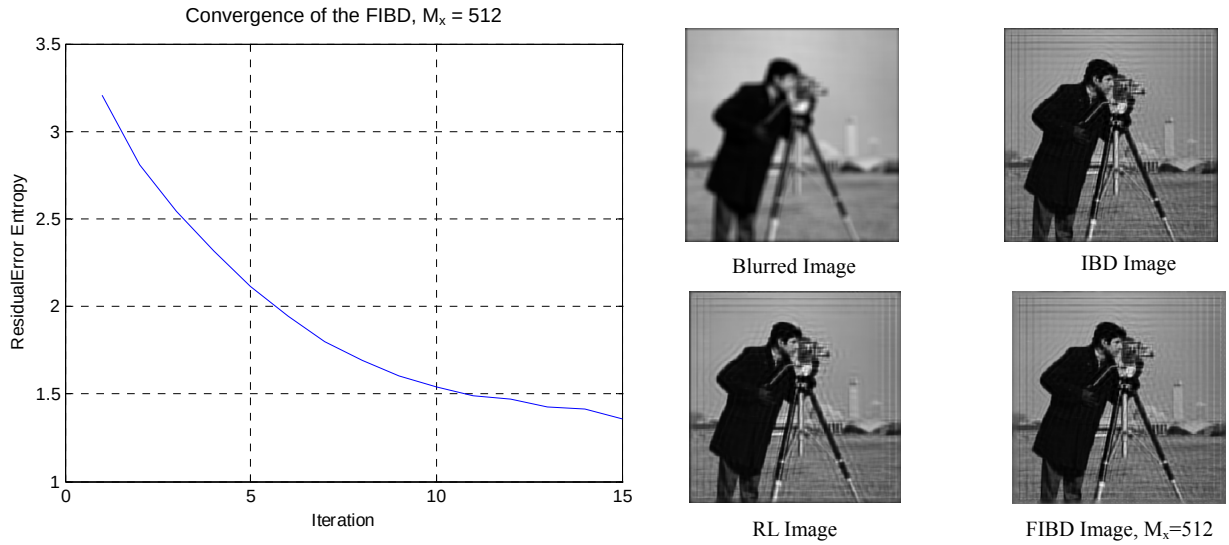

Figure 3. The rate of convergence as well as the deconvolved Cameraman images for Gaussian case.

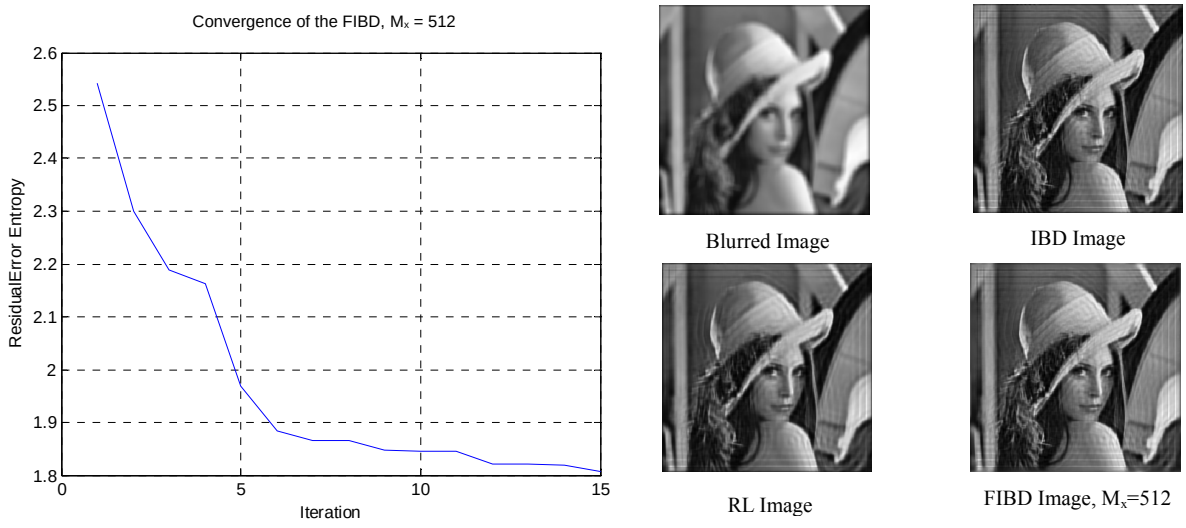

Figure 4. The rate of convergence as well as the deconvolved Lena images for Gaussian case.

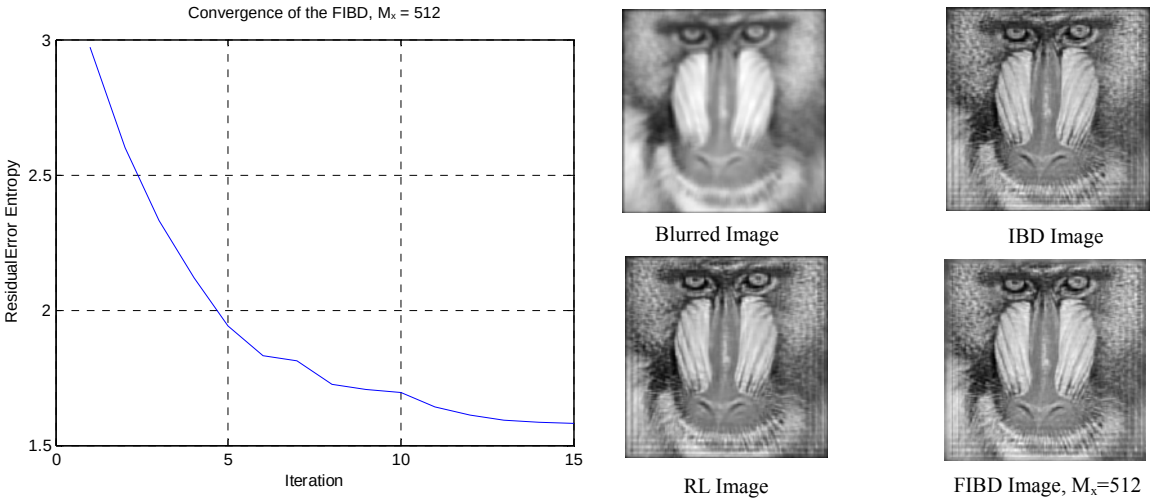

Figure 5. The rate of convergence as well as the deconvolved Mandril images for Gaussian case.

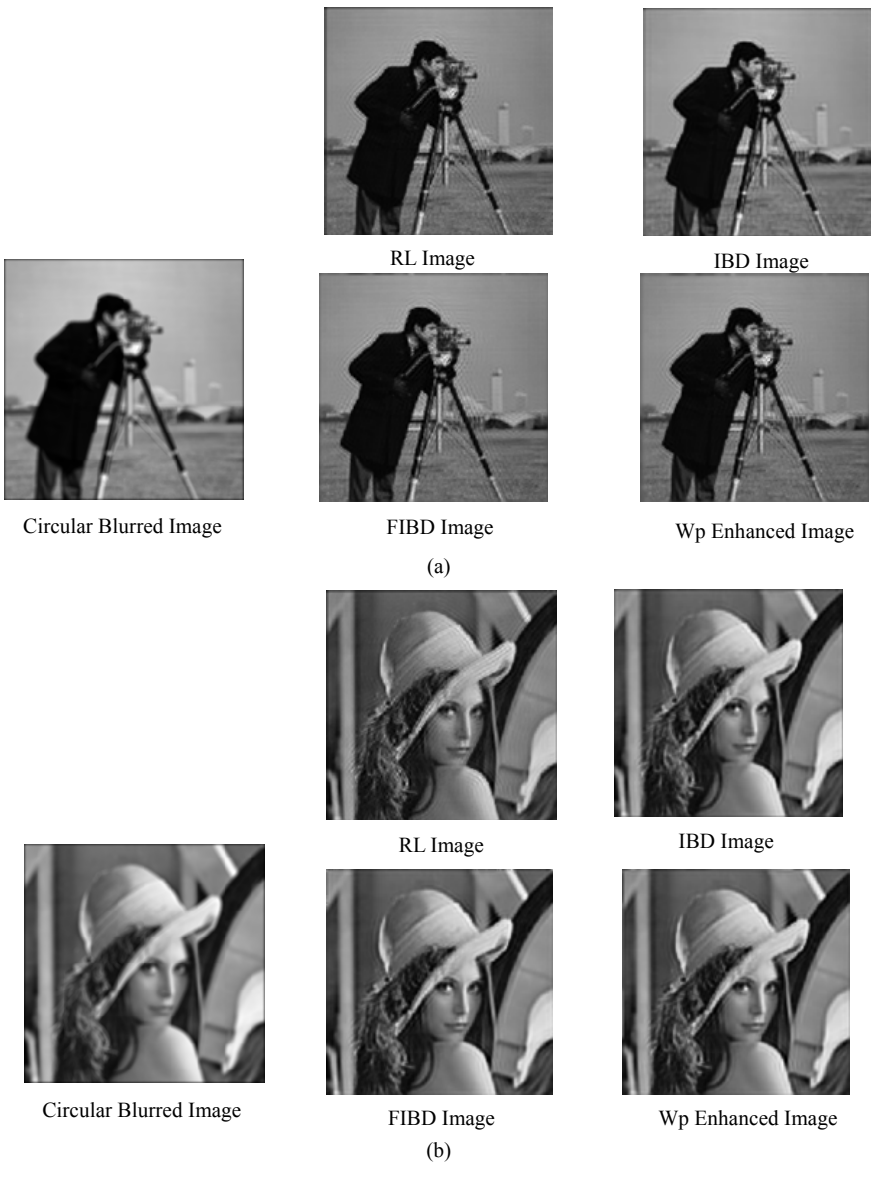

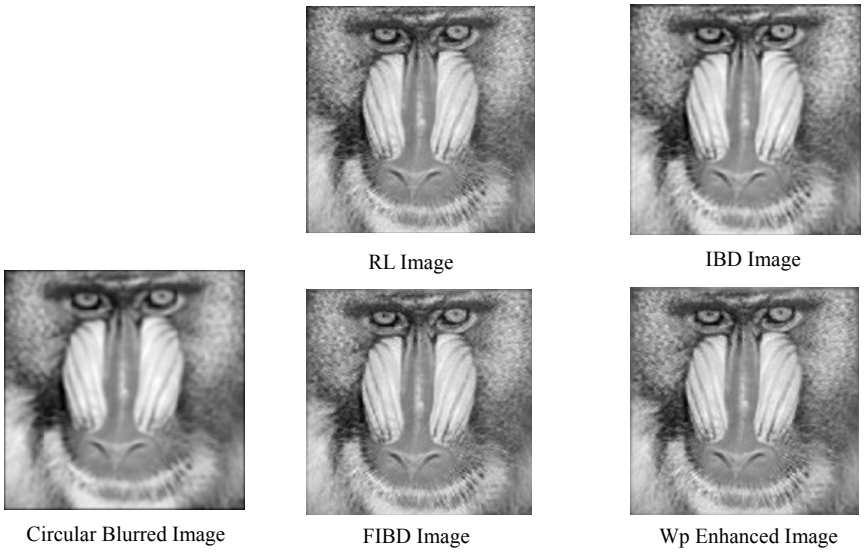

Figure 6. The blurring and deconvolved images.

the deconvolved image occurs.

3. Improving Sharpness of the Restoration Quality

As blurring affects the energies of the high frequency bands of the image, it is clear that deblurring should boost these high frequency energies. To explain this idea, consider the Matlab Cameraman image that is blurred using a Gaussian PSF of size 8 × 8 and $\sigma^2 = 10$. **Table 2** compares the percentage sub-band energies of 1-level "*Sym*4" wavelet decomposition, of the original Cameraman image, with those obtained for blurred, RL, IBD and the proposed FIBD deconvolved images. The FIBD image is obtained using M_x = 64. This table indicates that natural images have a significant amount of energy concentration in its *LL* sub-band. Moreover, blurring reduces the *LH*, *HL* and *HH* sub-bands. It also suggests that, the deblurred image quality can be improved through boosting the energies of the wavelet packets *LH*, *HL*, *HH*. This goal can be achieved by processing these sub-bands by a 2D mask H_0 that optimizes their energies while minimizing the residual energy of J_{er}. In order to reduce the effects of noise amplifications that predominates the *HH* sub-band, only the coefficients of the *LH* and *HL* are modified. The steps of the optimization algorithm can be summarized as follows:

1) Apply the *FIBD* algorithm to determine the optimum deconvolved image $\hat{f}^{(k)}(m,n)$, for the received blurred image $g(m, n)$.

2) Obtain the 1-level "*Sym*4" wavelet packet decomposition of $\hat{f}$.

3) For an arbitrary 2-D matrix H_0, normalize it to be a unity variance matrix, (*in order to avoid collapsing to zero in subsequent minimization steps*). Filter the packets *LH and HL* coefficients with H_0. Then, reconstruct the image from its modified wavelet packet using the synthesis bank to get $y(m, n)$. Evaluate the residual error

$$J_{er}(m,n) = g(m,n) - \sum_{r=0}^{N_1-1}\sum_{l=0}^{N_1-1}\hat{h}(r,l)\,y(m-r,n-l) \quad (12)$$

4) Using any unconstrained minimization algorithm, find the elements of H_0 that optimizes the detail packet energies while minimizing the error energy.

Tables 3(a) and **(b)** compare the PSNR improvements achieved with the classical IBD, FIBD as well as the Wave packet Optimized FIBD, using M_x = 64, 128, respectively when applying these steps to the above blurred images. In order to speed up computations, the 2-D mask H_0, is taken to be 4 × 4.

Edge improvements are checked by evaluating the norm of the difference between the exact edge of the original image, and the restored image edge. **Table 4** compares the edge improvement of the optimized FIBD with the RL and IBD restorations for Gaussian blurring PSF. This table indicates that, coupled with the PSNR improvement, except for the Mandril image, the proposed FIBD and its optimized wavelet version are sharper than RL and IBD counterparts. Thus, one can conclude that FIBD and its optimized wavelet version provide a superior deblurring image restoration technique. **Figures 6(a)-(c)**, compare the RL, IBD, FIBD and the optimized FIBD for the 3 Matlab images, with the FIBD technique for M_x = 64.

4. Conclusion

This paper, describes how, in blind deconvolution when

Table 2. % Sub-band energy concentration.

WP	Original	Blurred	RL	IBD	FEIBD
LL	99.2777	99.9890	99.7106	99.5414	99.6324
LH	0.2204	0.0049	0.1230	0.1883	0.1403
HL	0.4264	0.0061	0.1652	0.2680	0.2250
HH	0.0755	0.0000	0.0012	0.0023	0.0023

Table 3. (a) Wavelet packet PSNR improvement for Gaussian blurred images.

Blurring Type	IBD	FEIBD		Opt. FEIBD	
		64	128	64	128
Cameraman	23.6468	25.0114	25.1386	25.3257	25.3742
Lena	25.1177	25.6029	25.7005	25.4704	25.5538
Mandril	22,3211	23.1868	23.3061	23.3489	23.3914

Table 3. (b) Wavelet packet PSNR improvement for circular blurred images.

Blurring Type	IBD	FEIBD		Opt. FEIBD	
		64	128	64	128
Cameraman	25.6617	26.3235	26.4553	26.3346	26.4336
Lena	27.2219	27.5423	27.7395	27.0878	27.1839
Mandril	23.7927	24.3658	24.4249	24.3802	24.4237

Table 4. Edge error energy: Gaussian blurring.

Blurring Type	RL	IBD	WP Decomposition	
			64	128
Cameraman	53.6004	53.6656	51.9808	52.0000
Lena	52.4309	50.4480	49.3457	49.3254
Mandril	48.2804	48.4562	49.6588	49.7896

there is no priori information about both the true image and/or the blurring PSF, the size of the blurring PSF, can be accurately estimated for both noiseless and noisy blurred images. The paper also describes how using this estimated PSF size; the IBD or RL deconvolved images can be significantly improved. The proposed algorithms characterized by its fast convergence as a result of solving expressing pixels modifications as the solution of a set of linear equations. A novel method was also described to increase the sharpness of the deconvolved images. It remains to extend this work to the noisy case.

REFERENCES

[1] M. J. T. Smith and A. Docef, "A Study Guide for Digital Image Processing," Scientific Publishers Inc., Georgia, 1999.

[2] R. C. Gonzalez and R. E. Woods, "Digital Image Processing," 2nd Edition, Addison-Welsely Publishing Company, Reading, 1987.

[3] R. L. Lagendijk and J. Biemond, "Iterative Identification and Restoration of Images," Kluwer Academic Publishers, Boston, 1991. doi:10.1007/978-1-4615-3980-3

[4] G. R. Ayers and G. C. Danty, "Ierative Blind Deconvolution Method and Its applications," *Optics Letters*, Vol. 13, No. 7, 1988, pp. 547-549. doi:10.1364/OL.13.000547

[5] D. Kundur and D. Hatzinakios, "Blind Image Deconvolution Revisted," *IEEE Magazine on Signal Processing*, Vol. 13, No. 6, 1996, pp. 61-63.

[6] D. A. Fish, A. M. Brinicombe, E. R. Pike and J. G. Walker, "Blind Deconvolution by Means of the Richardson-Lucy Algorithm," *Journal of the Optical Society of America A*, Vol. 12, No. 1, 1995, pp. 58-65. doi:10.1364/JOSAA.12.000058

[7] D. S. C. Biggs and M. Andrews, "Acceleration of Iterative Image Restoration Algorithms," *Applied Optics*, Vol. 36, No. 8, 1997, pp. 1766-1775. doi:10.1364/AO.36.001766

[8] M. Jiang and G. Wang, "Development of Blind Image Deconvolution and Its Applications," *Journal of X-ray*

Science and Ology, Vol. 11, 2003, pp. 13-19.

[9] H. Y. Liu, Y. S. Zhang and J. I. Song, "Study on the Methods of Super Resolution Image Reconstruction," *The International Archives of the Photognanmetry*, *Remote Sensing and Spatial Information Science*, Vol. XXVII, Part B2, Beijing, 2008.

[10] D. Kundur and D. Hatzinakios, "Blind Image Deconvolution," *IEEE Magazine on Signal Processing*, Vol. 13, No. 3, 1996, pp. 43-64.

[11] S. Mallat, "A Wavelet Tour of Signal Processing, the Sparse Way," Academic Press, New York, 2009.

[12] M. F. Fahmy, G. M. Fahmy and O. M. Fahmy, "Bspline Wavelets in Signal De-Noising and Image Compression," *Journal of Signal, Image and Video Processing*, Vol. 5, No. 2, 2011, pp. 141-153. doi:10.1007/s11760-009-0148-x

